

# Analysis of the Proteomic Profile in Serum of Irradiated Nonhuman Primates Treated with Ex-Rad, a Radiation Medical Countermeasure

Alana D. Carpenter,<sup>#</sup> Yaoxiang Li,<sup>#</sup> Brianna L. Janocha, Stephen Y. Wise, Oluseyi O. Fatanmi, Manoj Maniar, Amrita K. Cheema, and Vijay K. Singh\*



Cite This: *J. Proteome Res.* 2023, 22, 1116–1126



Read Online

ACCESS |



Metrics & More



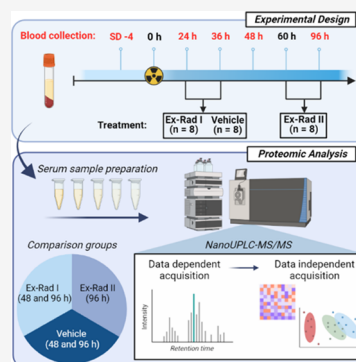
Article Recommendations



Supporting Information

**ABSTRACT:** There are currently four radiation medical countermeasures that have been approved by the United States Food and Drug Administration to mitigate hematopoietic acute radiation syndrome, all of which are repurposed radiomitigators. The evaluation of additional candidate drugs that may also be helpful for use during a radiological/nuclear emergency is ongoing. A chlorobenzyl sulfone derivative (organosulfur compound) known as Ex-Rad, or ON01210, is one such candidate medical countermeasure, being a novel, small-molecule kinase inhibitor that has demonstrated efficacy in the murine model. In this study, nonhuman primates exposed to ionizing radiation were subsequently administered Ex-Rad as two treatment schedules (Ex-Rad I administered 24 and 36 h post-irradiation, and Ex-Rad II administered 48 and 60 h post-irradiation) and the proteomic profiles of serum using a global molecular profiling approach were assessed. We observed that administration of Ex-Rad post-irradiation is capable of mitigating radiation-induced perturbations in protein abundance, particularly in restoring protein homeostasis, immune response, and mitigating hematopoietic damage, at least in part after acute exposure. Taken together, restoration of functionally significant pathway perturbations may serve to protect damage to vital organs and provide long-term survival benefits to the afflicted population.

**KEYWORDS:** *Ex-Rad, proteomics, rhesus macaque, total-body irradiation, radiation countermeasure, ON01210*



## INTRODUCTION

Radiological or nuclear exposure presents potential health and environmental hazards, risks that may be highlighted by larger, more devastating radiological/nuclear events.<sup>1–4</sup> The risk of radiation exposure following terrorists' radiological/nuclear weapons has posed an increasing concern.<sup>5,6</sup> Total- or partial-body exposure to ionizing radiation in sufficient doses at a high dose rate results in acute radiation syndrome (ARS), which is a potentially deadly illness that has limited treatment options. Clinical interventions to treat ARS include the administration of radiation medical countermeasures (MCMs) and other treatments depending on the absorbed radiation dose.<sup>7,8</sup> Despite extensive efforts over the last six decades to develop treatment options for ARS, only four MCMs including Neupogen, Neulasta, Leukine, and Nplate are currently approved by the United States Food and Drug Administration (US FDA) for the treatment of ARS and all four agents are repurposed radiomitigators.<sup>9–18</sup> Due to this deficit, additional MCMs must be developed to ensure an array of options are available in the Strategic National Stockpile/Vendor Managed Inventory for use in nuclear/radiological mass casualty scenarios.<sup>8</sup> Radiation MCMs that are safe, easily administered, and effective at reducing or eliminating adverse health consequences to individuals and the public are urgently needed to ensure an adequate level of nuclear and radiological preparedness.<sup>5,6,19</sup>

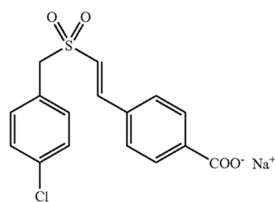
Several potential MCMs are currently under development, including the novel, small-molecule kinase inhibitor Ex-Rad, a chlorobenzyl sulfone derivative (organosulfur compound) that has received US FDA investigational new drug (IND) status.<sup>20,21</sup> This agent has been demonstrated to be an effective radiation MCM for hematopoietic as well as gastrointestinal acute radiation syndrome, and is effective through both parenteral and oral routes. Not only has Ex-Rad demonstrated significant protection against <sup>60</sup>Co gamma-irradiation when administered subcutaneously (sc, 500 mg/kg) to C3H/HeN mice 24 h and 15 min before irradiation with an estimated dose reduction factor of 1.16, Ex-Rad has also demonstrated significant survival benefit after prophylactic oral (po) administration.<sup>22,23</sup> Furthermore, Ex-Rad treatment appears to significantly limit hematopoietic and gastrointestinal injury within acutely irradiated rodents.<sup>22,24</sup> The objective of this study was to examine proteomic profiles that correlate with this agent as an oral radiomitigator in nonhuman primates (NHPs) with its administration delayed until at least 24 h after

Received: July 28, 2022

Published: March 28, 2023



irradiation. The drug dose selected was based on an allometric conversion of the dose tested in the murine model.



Chemical structure of Ex-Rad, C<sub>16</sub>H<sub>12</sub>ClNaO<sub>4</sub>S.

Understanding the mechanism by which Ex-Rad provides radiomitigation is key to optimizing its clinical application, which in turn supports the granting of IND status by the US FDA. One study demonstrated that the protective effects of Ex-Rad were manifested through the upregulation of the phosphatidylinositol 3-kinase (PI3K)/Akt (serine/threonine kinase, protein kinase B) pathways in cells exposed in vitro to ionizing radiation.<sup>25</sup> Another study has suggested that Ex-Rad acts by blocking ataxia-telangiectasia (ATM) and preventing the accumulation of p53 after exposure, which abrogates p-53-mediated programmed cell death.<sup>26</sup> Also, it was reported that Ex-Rad exerts its putative radioprotective efficacy by reducing the levels of pro-apoptosis proteins such as p53 and its downstream regulators p21, Bax, c-Abl, and p73, suggesting that Ex-Rad interferes with cellular damage that arises from ionizing radiation-induced p53-dependent apoptosis.<sup>22</sup> There is a report that AKT1 and AKT2 assist in the maintenance of hematopoietic stem cell function by regulating reactive oxygen species.<sup>27</sup> Recently, we have demonstrated using a global metabolomics molecular profiling approach with alterations in biochemical pathways relating to inflammation and oxidative stress in NHPs after irradiation that was alleviated by treatment with Ex-Rad.<sup>28,29</sup>

The objective of the study was to delineate proteomic profiles that correlate with the alleviation of radiation injury upon Ex-Rad administration. Additionally, we sought to understand the impact of treatment schedule on recovery as extrapolated from the resultant protein expression changes. To do this, NHPs were exposed to a single dose of 7.2 Gy (LD<sub>70/60</sub>) and were then split into three groups. The first group was administered vehicle, the second group was administered Ex-Rad 24 and 36 h post-irradiation (Ex-Rad I), and the third group was administered Ex-Rad 48 and 60 h post-irradiation (Ex-Rad II). Blood samples were collected at various time points pre- and post-irradiation, and serum was separated. For time points when the drug was administered and blood samples were collected on the same day (e.g., the 24 h time point), blood was collected prior to drug administration. Longitudinally collected serum samples were subjected to nano-LC-MS/MS-based proteomics analysis. Our results demonstrate that administration of Ex-Rad enables alleviation of radiation injury at least in part by reversing pathway perturbations caused by acute radiation exposure. We also observed that the Ex-Rad II group showed more robust reversal of the adverse effects of radiation exposure.

## MATERIALS AND METHODS

### Animals

For this study, the 24 male naïve rhesus macaques (*Macaca mulatta*, Chinese substrain) were acquired from the National Institutes of Health Animal Center (NIHAC, Poolesville, Maryland). All NHPs were 4–5 years old and weighed

between 4.3 and 6.2 kg. Upon being transferred to a vivarium accredited by the Association for Assessment and Accreditation of Laboratory Animal Care (AAALAC)-International, in which they were housed for the duration of the experiment, the animals underwent a 6-week quarantine period prior to the start of the study. Animal nutrition, housing, health monitoring, enrichment, and general care throughout the experimental period have previously been described in detail.<sup>30</sup> As irradiated animals are more prone to infection due to their suppressed immune system, paired housing was not possible during the experiment; however, the animals were able to see and touch neighboring animals through the cage divider. Single housing also prevents the possibility of conflict injuries that often occur in paired-housing arrangements. All animal-based procedures were approved (Protocol # P2013-12-016 approved on March 12, 2014) by the Institutional Animal Care and Use Committee (IACUC, Armed Forces Radiobiology Research Institute) and the Department of Defense Animal Care and Use Review Office (ACURO). This study strictly adhered to the recommendations within the Guide for the Care and Use of Laboratory Animals of the National Research Council of the National Academy of Sciences.<sup>31</sup> This study was carried out in compliance with the ARRIVE guideline.

### Experimental Design

The NHPs were randomly assigned to one of three treatment groups (eight NHPs per group) for this proteomic profiling study. The first group received the vehicle (at 24 and 36 h post-irradiation), the second group received Ex-Rad 40 mg/kg sc at 24 and 36 h post-irradiation, and the third group was administered 40 mg/kg of Ex-Rad sc at 48 and 60 h post-irradiation. As previously published, all animals were exposed to 7.2 Gy <sup>60</sup>Co gamma-radiation.<sup>28</sup> A total of 120 serum samples were collected from three groups at study day (SD) -4 and at 24, 36, 48, and 96 h post-irradiation. However, for the proteomic profile analyses, 3 total time points (48 and 96 h for Ex-Rad I and only 1 time point, 96 h for Ex-Rad II) were analyzed. It is of no value to assess the proteomic changes at 24 and 36 h for Ex-Rad I or 48 h for Ex-Rad II, as the drug was administered after sample collection at each time point.

### Drug Preparation and Administration

The drug preparation and administration have been described earlier.<sup>28</sup> Following irradiation, the NHPs were injected according to their assigned treatment regimen. The total dose administered was 40 mg/kg; the precise injection volume was calculated based on body weight at SD0 for each individual animal. At least 48 h prior to the scheduled drug administration, the injection site was shaved so that the skin could be easily monitored for any adverse reactions such as a rash, inflammation, irritation, or abscess formation. Immediately prior to drug injection, the injection site (the dorsal scapular region between the shoulder blades) was cleaned with 70% isopropyl alcohol and allowed to air dry. Ex-Rad or the vehicle was administered sc using a sterile 21–24-gauge needle attached to a 3–6 mL disposable luer-lock syringe.

### Radiation Exposure

Dose rate measurement was performed as previously described prior to irradiation.<sup>32,33</sup> Upon arrival at the Cobalt Facility, animals were sedated with ketamine hydrochloride (10–15 mg/kg intramuscular (im)) to limit movement and distress during the procedure. The NHPs were irradiated in pairs,

based on abdominal widths measured with digital calipers. This would ensure that the animals would be delivered a precise total-body midline dose of 7.2 Gy  $^{60}\text{Co}$  gamma-radiation at a rate of 0.6 Gy/min. Each animal was secured in an individual restraint device, which was placed onto the irradiation platform facing away from one another. While undergoing the procedure, the NHPs were continuously observed using a real-time video monitoring system. Once the animals were determined to be in a stable condition following the procedure, they were transported back to the vivarium in the same manner as they arrived. The animals were regularly monitored to ensure a complete, complication-free recovery from sedation.

The alanine/EPR (electron paramagnetic resonance) system was used for dosimetry, which is widely accepted as one of the most accurate methods for measuring relatively high radiation doses to date.<sup>33–35</sup> The dose measurements at the Armed Forces Radiobiology Research Institute (AFRRI) used calibration curves (EMXmicro spectrometer, Bruker Corp., Billerica, Massachusetts) based on the standard alanine calibration sets purchased from the US National Institute of Standards and Technology (NIST, Gaithersburg, Maryland). Prior to their use, the alanine dosimeters were calibrated in terms of absorbed dose to water using the US National Standard Radiation Sources. Identical alanine dosimeters were placed with the NHP phantoms (Plexiglas cylinders 6.9, 10, 12.5 cm in diameter, and 34.5 cm in length) on the irradiation platform, and were irradiated to approximately 100 Gy. The EPR signals were then measured to determine the dose rates to water, which were then adjusted to account for the difference in mass energy absorption coefficients between water and the soft tissue of NHPs.

### Serum Sample Collection

Animals were handled via the pole-and-collar method to secure them in a custom-made restraint chair for blood collection as described earlier.<sup>28</sup> Once collected, the blood was placed in serum-separating tubes and allowed to clot for at least 30 min prior to being centrifuged (10 min, 400g). The serum was aliquoted into empty specimen tubes which were then stored at  $-70\text{ }^{\circ}\text{C}$  until use.

The blood samples collected 24 h post-irradiation were collected just prior to the first dose of Ex-Rad administration to the Ex-Rad I group. Similarly, samples collected at 36 h from the Ex-Rad I group were taken just prior to the administration of the second dose of Ex-Rad to this group. Lastly, samples collected at 48 h post-irradiation were collected just before the administration of the first dose of Ex-Rad to Ex-Rad II group animals. In brief, blood samples for serum collection were collected prior to drug administration at each time point, and samples were collected at SD-4, and 24, 36, 48, and 96 h post-irradiation for proteomic analysis. Thus, although drug administrations occurred at 24 and 36 h for Ex-Rad I, and at 48 and 96 h for Ex-Rad II, the statistically significant effects of Ex-Rad I can only be studied at 48 and 96 h, while the effects of Ex-Rad II can only be viewed at 96 h.

Blood samples were collected for serum biochemistry analysis at SD-4, 36 h, 60 h, and SD6. Parameters evaluated included albumin, alanine transaminase (ALT), alkaline phosphatase (ALKP), aspartate transferase (AST), glucose, total bilirubin, total protein, gamma-glutamyl transferase (GGT), creatinine, calcium, chloride, potassium, sodium, and uric acid.

### Serum Sample Preparation for Proteomics Analysis

A serum volume of 25  $\mu\text{L}$  was diluted five times with load/wash buffer solution (Agilent Cat. #: 5185-5987) and mixed for 30 s. Each sample was filtered through a 0.22- $\mu\text{m}$  spin filter (Agilent Cat. #: 5185-5990) for 2 min at 16,000g. Multiple affinity removal system (MARS14, Agilent Cat. #: 5188-6557) columns ( $4.6 \times 50\text{ mm}^2$ ) were used to deplete the most abundant 14 proteins in serum according to the manufacturer protocol on a Waters Acquity HPLC system.<sup>36</sup> Protein peaks were selectively collected and transferred to Spin Concentrators, 5 K MWCO, 4 mL capacity (Agilent Cat. #: 5185-5991) and centrifuged at 17,172g for 45 min at  $4\text{ }^{\circ}\text{C}$ . A volume of 1 mL of liquid chromatography–mass spectrometry (LC-MS)-grade water was added to the concentrated sample and centrifuged at 17,172g for 45 min at  $4\text{ }^{\circ}\text{C}$  to wash out salts and this process was repeated one more time. A volume of 1 mL of 50 mM ammonium bicarbonate solution (pH of approximately 8) was used to rebuffer each sample of concentrated proteins. The final protein concentration was determined using a BCA protein assay kit (Thermo Fisher Scientific Cat. #: 23227).<sup>36</sup>

Protein concentration was adjusted to 40  $\mu\text{g}/100\text{ }\mu\text{L}$  in 50 mM ammonium bicarbonate buffer, reduced with dithiothreitol (DTT) to a final concentration of 5 mM for 60 min at  $56\text{ }^{\circ}\text{C}$  and alkylated with iodoacetamide to a final concentration of 15 mM for 30 min at  $37\text{ }^{\circ}\text{C}$  in a dark environment with Lys-C (Promega, Cat. # V1671) at 1:100 (w/w) enzyme-to-protein ratio for 3 h at  $37\text{ }^{\circ}\text{C}$ . Trypsin Gold (Promega, Cat. # V5280) was added to a final 1:50 (w/w) enzyme-to-protein ratio for overnight digestion at  $37\text{ }^{\circ}\text{C}$  for 16 h, to complete the reaction. Trypsin and Lys-C enzymes were deactivated by heating at  $90\text{ }^{\circ}\text{C}$  for 10 min and samples were allowed to cool down to room temperature and then acidified to a pH = 3 using 0.1% trifluoroacetic acid in water.<sup>36</sup> The digested peptides were purified on microspin C18 columns (The Nest Group, Inc., HEM S18V) and eluted using  $1 \times 400\text{ }\mu\text{L}$  of 80%  $\text{H}_2\text{O}$  acidified by 0.1% formic acid followed by  $1 \times 400\text{ }\mu\text{L}$  of 50% ACN/ $\text{H}_2\text{O}$  acidified by 0.1% formic acid. The collected fractions were evaporated under vacuum and reconstituted for LC-MS for data-independent acquisition (DIA) analysis.

### Blood Chemistry Analysis

Various blood biochemistry parameters were analyzed from serum samples obtained at SD-4, 36 h, 60 h, and SD6. Samples from all treatment groups were pooled for each time point, and the pre-irradiation time point was compared to the 36 h, 60 h, and SD6 time points to assess the effects of radiation.

### Serum Proteomics Using NanoUPLC-MS/MS

A sample pool from all of the subjects (with an equal amount of protein extracts combined) was prepared to establish a protein library of all serum proteins detectable with tandem mass spectrometry (MS/MS). The pooled peptide sample was fractionated with a  $2.1 \times 150\text{ mm}^2$  column XTerra MS C18 column (Waters) on an Agilent Infinity II HPLC instrument equipped with a Diode Array Detector HS detector in high-pH reversed-phase chromatography mode. Solvent A (2% acetonitrile, 4.5 mM ammonium formate, pH = 10) and a nonlinear increasing concentration of solvent B (90% acetonitrile, 4.5 mM ammonium formate, pH = 10) were used to separate peptides. The 95-min separation LC gradient followed this profile: (min: %B) 0:2; 5:5; 70:50; 75:75; 80:100; 90:2; and 95: 2. The flow rate was 0.2 mL/min. A total of 20 fractions were obtained in a step-wise concatenation



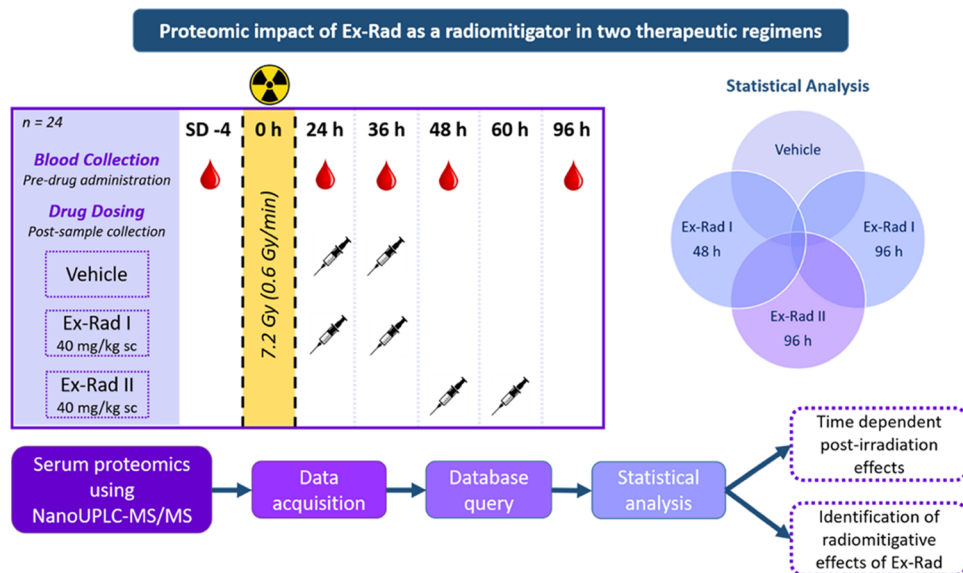


**Figure 1.** Overall experimental design for biomarker discovery of radiation exposure and Ex-Rad I and Ex-Rad II treatments. Figure was created by the author using Microsoft PowerPoint (URL: <https://www.microsoft.com/en-us/microsoft-365/powerpoint>).

strategy, followed by acidification to a final concentration of 0.1% formic acid and dried down with a SpeedVac.<sup>36</sup>

### Data Acquisition

Nano-liquid chromatography-tandem mass spectrometry (nano-LC-MS/MS) was used to analyze the peptides from human serum digests, performed on a ThermoFisher Ultimate 3000 HPLC System (Thermo Fisher Scientific, Bremen, Germany) connected to a quadrupole-Orbitrap mass spectrometer (Q-Exactive, Thermo Fisher Scientific, Bremen, Germany) equipped with an online nano-electrospray flex ion source.

First, the peptides were redissolved in 40  $\mu\text{L}$  of solvent (100% water with 0.1% formic acid) and then 1  $\mu\text{g}$  peptide sample was loaded on the analytical column (Acclaim PepMap C18, 75 mm and 25 cm). Subsequently, the peptides were separated and identified under a 65 min method, which was composed of 2 min in 25% B, 40 min of 95% B, 48 min of 95% B, 50 min of 1% B, 50.1 min of 95% B, 55 min of 95%, and 57 min of 1% B. The column was then reequilibrated at initial conditions for 8 min with a constant flow rate of 300 nL/min. The column temperature was kept at ambient temperature and the electrospray voltage of 2.2 kV vs the inlet of the mass spectrometer was applied. For the library development on the fractions, the Q-Exactive mass spectrometer was operated in data-dependent mode and each scan cycle consisted of one full-MS scan at the  $m/z$  ranging from  $m/z$  375–2000 with a mass resolution of 70 K. Then, the selected parent ions were fragmented in ten sequential high-energy collisional dissociations (HCD) MS/MS scans with a resolution of 17.5 K. In addition, for MS/MS, the precursor ions were activated with 30% normalized collision energy and 2  $m/z$  of the isolation window. In all cases, single charge state was rejected and a micro-scan was recorded using dynamic exclusion of 30 s.

Samples were acquired in the data-independent acquisition (DIA) mode after a full precursor ion scan (range between 375–2000  $m/z$ ). The resolution of the instrument was set to 35,000 and the isolation window was 20 Da. For both data-dependent acquisition (DDA) and DIA, the normalized collision energy (NCE) was 30 eV.

### Database Retrieval and Statistical Tests

Tandem mass spectra were searched by Pulsar search engine (Biognosys) and the database searched was the Human UniProt obtained on Nov 23, 2021. The data retrieval parameters for the Q-Exactive instrument were as follows: precursor mass tolerance: 5 ppm; fragment mass tolerance: 50 mmu; enzyme: trypsin; missed cleavages: 2; fixed modification: carbamidomethyl on cysteine (C); variable modifications: oxidation on methionine (M). The percolator algorithm was used to control the false discovery rate (FDR) of peptides below 1%.

The test of radiation effect and radiomitigative effects of Ex-Rad were calculated either by Mann–Whitney U test or two-tailed unpaired Student  $t$ -test, whereas  $p$ -values of less than 0.05 exclusively were considered significant. Furthermore,  $p$ -values were corrected for multiple testing using Benjamini–Hochberg procedure which limits the FDRs. All statistical analyses were performed using R (version 4.2.0).

For blood chemistry data, mean values with standard errors are reported. A one-way ANOVA test was performed to detect statistically significant differences between the vehicle group and either the Ex-Rad I or II groups. Due to minimal significant differences between treatment groups, an unpaired two-tailed  $t$ -test was performed on pooled data from each group at every time point. Pooled data from the post-irradiation time points were compared to the pre-irradiation baseline to collectively view the overall effects of irradiation on blood biochemistry.

## RESULTS

Ex-Rad is a promising radiation MCM with hematopoietic and gastrointestinal radioprotective efficacy and has shown to be orally effective in murine models.<sup>22–24,26,37</sup> Since the treatment schedule in relation to radiation exposure is crucial for ARS MCM development, we investigated two treatment regimens and used proteomic profiles as a read out of alleviation of radiation injury. Therefore, the NHPs were randomly divided into 3 different treatment groups and were then exposed to a single dose of 7.2 Gy of <sup>60</sup>Co gamma-radiation prior to drug



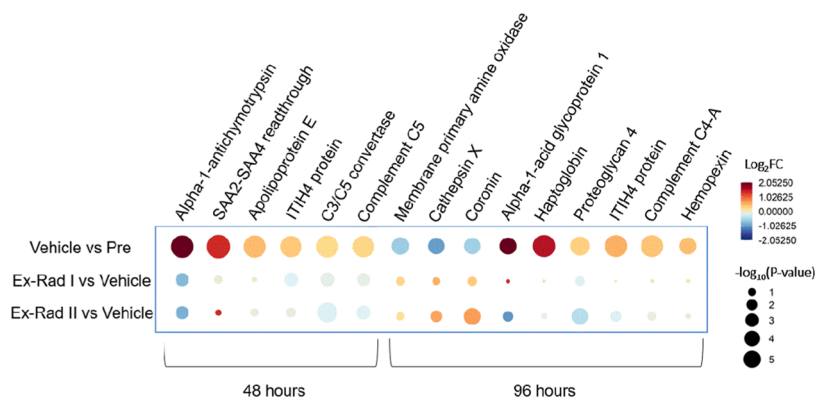


**Figure 4.** Raindrop plot demonstrating the radiomitigative effects of Ex-Rad on various proteins at 48 and 96 h post-irradiation. Figure was created by open-source software R (version 4.2.0, URL: <https://cran.r-project.org/>).

irradiated groups at 24 and 36 h post-exposure (Figure 2). A two-dimensional (2D) score plot comparing data collected at 24 h to the pre-irradiation time point was constructed (Figure 2A), as well as a three-dimensional (3D) score plot comparing protein expression 36 h post-irradiation to the pre-irradiation values (Figure 2B). Volcano plots, which reveal the peak intensities of each protein at 24 and 36 h compared to pre-irradiation, were constructed to view the overall pattern of annotated proteins and can be viewed in Figure 3A,B, respectively.

Proteins that were found to be significantly dysregulated were then isolated and used as input for the Reactome Pathway Database (URL: <https://reactome.org>) to detect common pathways involved. Results were then projected to human data, due to the high percent homology between humans and NHPs and the small number of reviewed proteins in the rhesus macaque database compared to the well-supported human database. It was observed that the hemostasis; innate immune system; platelet degranulation; platelet activation, signaling, and aggregation; response to elevated platelet cytosolic  $Ca^{2+}$ ; signal transduction; neutrophil degranulation; metabolism of proteins; regulation of insulin-like growth factor (IGF) transport and uptake by insulin-like growth factor binding proteins (IGFBPs); and disease pathways were dysregulated at all time points, suggesting these pathways are sensitive to radiation-induced perturbations. Data at 24, 36, 48, and 96 h post-irradiation compared to the pre-irradiation time point can be viewed in Supporting Table 1.

#### Treatment with Ex-Rad Partially Reversed Irradiation-Induced Proteomic Changes

Significantly dysregulated proteins in the Ex-Rad I and II groups were delineated to determine the radiomitigative effects of either treatment group on protein expression. Serum collected from the vehicle group was compared to serum collected from the Ex-Rad I group at 36 h (only one dose of the drug had been administered at this time point since blood was collected immediately prior to drug administration), 48, and 96 h, and in the Ex-Rad II group, only at 96 h. Statistical analysis was performed on all samples collected. However, because drug administrations occurred at 24 and 36 h for Ex-Rad I and at 48 and 96 h for Ex-Rad II, in-depth analysis of the radiomitigative effects of Ex-Rad is restricted to only a few time points. The statistically significant effects of Ex-Rad I can only be viewed at 48 and 96 h, while the effects of Ex-Rad II can only be viewed at 96 h. Proteins whose post-irradiation concentrations are less altered compared to baseline values are

included for Ex-Rad I at 48 and 96 h (Supporting Tables S3 and S4, respectively) and for Ex-Rad II at 96 h (Supporting Table S5).

At the 36 h time point for Ex-Rad I (after only one drug dose), radiation-induced perturbations in 11 proteins were significantly mitigated. By the 48 h serum collection time point (after both doses of the drug), the circulating levels of 20 proteins were found to be significantly reversed to near-normal abundance, suggesting possible mitigation by Ex-Rad administration post-irradiation. Lastly, at 96 h post-irradiation (60 h after the second dose of the drug), the effects of radiation exposure were mitigated in 11 proteins in contrast to the vehicle-treated group. As previously mentioned, the 96 h time point was analyzed for Ex-Rad II (36 h after the second dose of the drug, which was administered at 60 h), which revealed that radiation-induced perturbations were significantly mitigated in a total of 41 proteins. Comparisons were then made across these time points to determine which pathways were up or downregulated, and which pathways were inhibited in an effort to understand the action of ionizing radiation mechanistically.

At 48 h post-irradiation in the Ex-Rad I group, 20 total proteins were found to be significantly mitigated by Ex-Rad treatment, with 12 proteins downregulated and 8 proteins upregulated. At 96 h post-irradiation in this group, a total of 5 proteins were downregulated and 6 proteins were upregulated. Concentrations of 41 proteins were significantly perturbed in the Ex-Rad II group (analyzed at the 96 h time point) following irradiation; 23 were upregulated and 18 were downregulated. Proteins significantly mitigated post-irradiation were again entered into the Reactome Pathway Database, and several common pathways were found to be significantly dysregulated at all time points used for analysis.

**Immune System Pathway.** Perturbations in protein concentrations linked to various pathways were found to be mitigated by Ex-Rad administration at the 48 and 96 h time points (Figure 4). It is important to note that at 48 h post-irradiation, the Ex-Rad I group had been administered both doses of Ex-Rad, while the Ex-Rad II group had only been administered one dose. For the 96 h time point, both doses of Ex-Rad had been administered to the Ex-Rad I and II groups. The dysregulation of several proteins linked to immune system pathways was found to be mitigated by Ex-Rad in both drug administration schedules. At 48 h post-irradiation, radiation-induced dysregulation to proteins including complement C5, C3/C5 convertase, ITIH4 protein, and  $\alpha$ -antichymotrypsin was significantly mitigated by both doses of Ex-Rad I compared

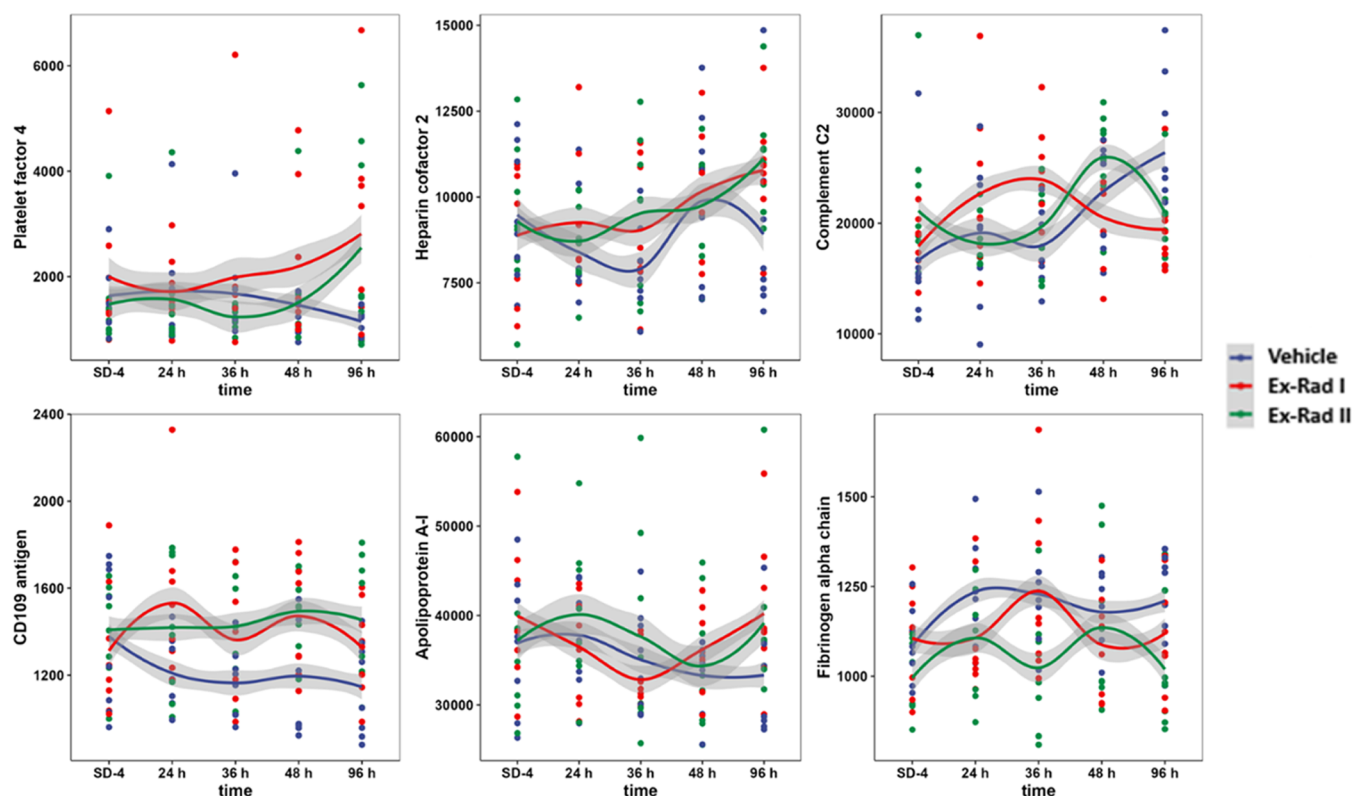


**Figure 5.** Trend lines comparing NHP serum profiles at SD-4 (pre-irradiation), 24, 36, 48, and 96 h for vehicle, Ex-Rad I, and Ex-Rad II, separately. The y-axis represents the normalized intensity of the selected proteins. Constant distances between time points were chosen for clarity. The shaded area in the plot is intended to represent data dispersion, which was calculated using the locally estimated scatterplot smoothing (LOESS). The width of the shaded area is consistent with the 50% confidence interval of the trendline, which is applied to all proteins in the figure. It is important to note that the x-axis in this representation is solely for observing protein trends and does not carry any statistical significance. Figure was created by open-source software R (version 4.2.0, URL: <https://cran.r-project.org/>).

to the vehicle group. Interestingly, mitigation was also seen in the Ex-Rad II group to a lesser extent, which had only received one dose of Ex-Rad at this time point. At the 96 h time point, dysregulation in hemopexin, complement C4-A, ITIH4 protein, cathepsin X, and coronin were found to be mitigated by both Ex-Rad administration schedules. However, it is important to note that at the 96 h time point, it had been 60 h since the Ex-Rad I group was administered its last dose, and only 36 h since the Ex-Rad II group was administered its last dose. Other notable proteins were also linked to immune system pathways. Sulfhydryl oxidase 1 and platelet basic protein were upregulated, while plasmin-2 was downregulated. At 96 h post-irradiation in Ex-Rad I, complement C2 was downregulated and was linked to the activation of the C3 and C5 pathways. At 96 h post-irradiation in the Ex-Rad II group, apolipoprotein B-100, desmoglein-1, fructose-bisphosphate aldolase C, and monocyte differentiation antigen CD14 were upregulated, and complement C4-B, fibrinogen  $\alpha$  chain, catalase, and plasmin-2 were downregulated (Supporting Tables S6–S9).

**Hemostasis Pathway.** Proteins involved in the hemostasis pathway were altered post-irradiation in both treatment groups at all time points analyzed. At 48 h post-irradiation, proteins including sulfhydryl oxidase 1 and platelet basic protein were both significantly upregulated. At 96 h post-irradiation in the Ex-Rad I group, two proteins (platelet factor 4 and coagulation factor IX) were also significantly upregulated. Lastly, at 96 h post-irradiation in the Ex-Rad II group compared to the

vehicle-treated group, a greater number of proteins related to hemostasis were activated compared to the Ex-Rad I time points. Proteins including apolipoprotein B-100, heparin cofactor 2, galectin-3-binding protein,  $\beta$ -2-glycoprotein 1, and CD109 antigen were significantly upregulated, while fibrinogen  $\alpha$  chain, fermitin family homolog 3, thymosin  $\beta$ -4, and transgelin-2 were significantly downregulated (Supporting Tables S6–S9). Radiation-induced damage was found to be mitigated by Ex-Rad treatment by a return to near baseline levels (SD-4) compared to the 96 h time point. At 96 h post-irradiation, dysregulation in coronin was found to be mitigated in the Ex-Rad I treatment group, while dysregulation in hemopexin and haptoglobin was found to be mitigated in both treatment groups (Figure 4). Proteins linked to hemostasis pathways including platelet factor 4, heparin cofactor 2, and fibrinogen  $\alpha$  chain demonstrated a return to near baseline levels with Ex-Rad treatment, indicating that Ex-Rad plays an important role in sparing these pathways to radiation injury (Figure 5).

Multivariate analysis showed that 20 annotated proteins reverted back to near pre-irradiation abundance with the Ex-Rad I treatment approach, while a total of 41 proteins showed a similar reversal effect with the Ex-Rad II treatment schedule. Some of the most notable proteins affected can be viewed in trend line concentrations for these proteins in Ex-Rad I, Ex-Rad II, and vehicle-treated groups over the course of the study in Figure 5. The outcome of this analysis revealed that both treatment schedules were successful at mitigating radiation-



induced perturbations in protein expression; however, the Ex-Rad II treatment schedule provided a more robust amelioration of radiation-induced damage to proteomic pathways. For the most part, the same pathways were affected by both Ex-Rad I and II treatment schedules; however, different proteins were linked to the same pathways, with a lower number of proteins linked to a specific pathway in the Ex-Rad I group, and a larger number of proteins in the Ex-Rad II group, emphasizing higher significance to the latter group. Additional pathways were mediated by both treatment schedules including metabolism, metabolism of proteins, sensory perception, signal transduction, transport of small molecules, and disease pathways that were affected by Ex-Rad I treatment, while the gene expression (transcription), transport of small molecules, metabolism of proteins, vesicle-mediated transport, cell cycle, disease, and programmed cell death pathways were affected by Ex-Rad II treatment. An exhaustive list of all data for each treatment group comparison at each time point can be viewed in [Supporting Tables S6–S9](#).

### Serum Biochemistry

All treatment groups generally followed similar trends in each parameter throughout the study, with minimal deviation between the drug and vehicle-treated groups apart from a few isolated time points. Significant changes in serum blood chemistry were found in several parameters when pooling data from all treatment groups, and comparing the pre-irradiation time point to the post-irradiation time points. Radiation was found to induce significant changes in at least one time point in all parameters, apart from uric acid. These data are available for reference in [Supporting Figure S1](#).

## DISCUSSION

The purpose of this study was to assess the radiomitigative potential of two different dosing schedules of Ex-Rad by evaluating its ability to mitigate radiation-induced perturbations in protein abundance following acute exposure to ionizing radiation. Global proteomic profiling of serum samples collected at various time points pre- and post-irradiation was accomplished using a nanoUPLC-MS/MS technique to analyze the effects of radiation on protein abundance and the subsequent recovery afforded by Ex-Rad.

The results of this study suggest that both administration schedules reversed radiation-induced alterations in serum protein abundance. Significantly dysregulated proteins were compared at the 48 and 96 h time points for Ex-Rad I and the 96 h time point for Ex-Rad II. Although there was a significant overlap in the pathways that reverted to homeostasis with both dosing regimens, radiation-induced perturbations in a greater number of proteins were significantly restored by the treatment schedule of Ex-Rad II (48 and 60 h post-irradiation of Ex-Rad administration) compared to Ex-Rad I (24 and 36 h post-irradiation Ex-Rad administration). Recently, we have demonstrated restoration of irradiation-induced proteomic alterations using a few promising radiation MCMs under development; gamma-tocotrienol,<sup>38</sup> tocopherol succinate,<sup>39</sup> and BIO 300<sup>40</sup> in murine and NHP models.<sup>36,41,42</sup> There is another report demonstrating a robust alteration by gamma-tocotrienol in spleen proteomic profiles including upregulation of the Wnt signaling pathway and actin-cytoskeleton linked proteins in mediating the radiation injury in mice, which suggests that pretreatment with gamma-tocotrienol attenuated radiation-induced injury in the spleen by modulating various cell

signaling proteins.<sup>43</sup> This current study also confirms the restoration of radiation-induced proteomic alterations by Ex-Rad treatment, albeit by different mechanistic pathways. The results of this study suggest that Ex-Rad may exert its radiomitigative effects by restoring pathways involved in hemostasis and immune system regulation. This is significant since radiation-induced immune system dysregulation has been implicated in chronic inflammation and accelerated aging processes in the A-bomb survivors.<sup>44</sup> Radiation is known to activate the coagulation cascade and induce changes in hemostasis pathways that are essential for controlling hemorrhage. This is significant since macromolecular damage is known to impact several downstream molecular events including DNA damage, endoplasmic reticulum stress/unfolded protein response, cell cycle arrest, cell death, and senescence.<sup>45</sup>

Recently, we have reported the metabolomic and lipidomic profiles in serum samples of NHPs treated with Ex-Rad I and Ex-Rad II and compared these with vehicle-treated control animal serum samples.<sup>28,46</sup> We observed alterations in biochemical pathways relating to inflammation and oxidative stress after radiation exposure that were alleviated in animals receiving Ex-Rad I or Ex-Rad II. It is important to note that similar to the current proteomic study results, irradiation-induced metabolic dysregulation was alleviated by Ex-Rad treatment. Specifically, the Ex-Rad II treatment alleviates such changes better compared to Ex-Rad I treatment.<sup>28</sup> We have also demonstrated that dysregulated metabolites induced by irradiation were alleviated in NHPs by the treatment of other MCMs under development, such as BIO 300<sup>47</sup> and gamma-tocotrienol.<sup>32</sup>

## CONCLUSIONS

Taken together, the results of our study suggest that Ex-Rad is capable of mitigating radiation-induced perturbations in protein abundance, regardless of treatment schedule; however, Ex-Rad administered at 48 and 60 h post-irradiation provided the most significant benefit. Due to the timing of blood collections, the effects of the first dose of Ex-Rad at 48 h post-irradiation in Ex-Rad II could not be observed. Additionally, the effects of two doses of Ex-Rad at 48 and 60 h post-irradiation in Ex-Rad II could not be observed past 96 h post-irradiation. These limitations in sample collection timing prevented additional insights into the pathways in which this treatment schedule works to mitigate radiation-induced damage to protein abundance. Regardless, additional studies are needed to determine the mechanistic pathways in which Ex-Rad restores protein abundance post-irradiation. Understanding the mechanism of injury and the pathways involved in radiation injury and the MCM's mechanism of action are vital to MCM development and regulatory approval by the US FDA following Animal Rule.<sup>14,48,49</sup>

## ASSOCIATED CONTENT

### Data Availability Statement

All data generated or analyzed during this study are included in this published article (and its [Supporting Information](#) files).

### Supporting Information

The Supporting Information is available free of charge at <https://pubs.acs.org/doi/10.1021/acs.jproteome.2c00458>.

UniProt IDs, protein names, and gene names (Table S1); comprehensive data of the effects of radiation at



different time points (Table S2); comprehensive list of proteins that are less altered by radiation at 48 h compared to baseline values due to the administration of Ex-Rad I (administered at 24 and 36 h post-irradiation) (Table S3); comprehensive list of proteins that are less altered by radiation at 96 h compared to baseline values due to the administration of Ex-Rad I (administered at 24 and 36 h post-irradiation) (Table S4); comprehensive list of proteins that are less altered by radiation at 96 h compared to baseline values due to the administration of Ex-Rad II (administered at 48 and 60 h post-irradiation) (Table S5); comparison of the effects of radiation at 24 h post-irradiation (Table S6); comparison of the effects of radiation at 36 h post-irradiation (Table S7); comparison of the effects of radiation at 48 h post-irradiation (Table S8); comparison of the effects of radiation at 96 h post-irradiation (Table S9); and albumin, ALT, ALKP, AST, glucose, total bilirubin, total protein, GGT, creatinine, calcium, chloride, potassium, sodium, and uric acid concentrations on SD-4, 36 h, 60 h, and SD6 in the vehicle, Ex-Rad I, and Ex-Rad II-treated groups (PDF)

## AUTHOR INFORMATION

### Corresponding Author

**Vijay K. Singh** – *Division of Radioprotectants, Department of Pharmacology and Molecular Therapeutics, F. Edward Hébert School of Medicine, Uniformed Services University of the Health Sciences, Bethesda, Maryland 20814, United States; Armed Forces Radiobiology Research Institute, Uniformed Services University of the Health Sciences, Bethesda, Maryland 20814, United States; [orcid.org/0000-0002-6631-3849](https://orcid.org/0000-0002-6631-3849); Phone: 301-295-2347; Email: [vijay.singh@usuhs.edu](mailto:vijay.singh@usuhs.edu)*

### Authors

**Alana D. Carpenter** – *Division of Radioprotectants, Department of Pharmacology and Molecular Therapeutics, F. Edward Hébert School of Medicine, Uniformed Services University of the Health Sciences, Bethesda, Maryland 20814, United States; Armed Forces Radiobiology Research Institute, Uniformed Services University of the Health Sciences, Bethesda, Maryland 20814, United States*

**Yaoliang Li** – *Department of Oncology, Lombardi Comprehensive Cancer Center, Georgetown University Medical Center, Washington, District of Columbia 20057, United States*

**Brianna L. Janocha** – *Division of Radioprotectants, Department of Pharmacology and Molecular Therapeutics, F. Edward Hébert School of Medicine, Uniformed Services University of the Health Sciences, Bethesda, Maryland 20814, United States; Armed Forces Radiobiology Research Institute, Uniformed Services University of the Health Sciences, Bethesda, Maryland 20814, United States*

**Stephen Y. Wise** – *Division of Radioprotectants, Department of Pharmacology and Molecular Therapeutics, F. Edward Hébert School of Medicine, Uniformed Services University of the Health Sciences, Bethesda, Maryland 20814, United States; Armed Forces Radiobiology Research Institute, Uniformed Services University of the Health Sciences, Bethesda, Maryland 20814, United States*

**Oluseyi O. Fatanmi** – *Division of Radioprotectants, Department of Pharmacology and Molecular Therapeutics, F. Edward Hébert School of Medicine, Uniformed Services University of the Health Sciences, Bethesda, Maryland 20814, United States; Armed Forces Radiobiology Research Institute, Uniformed Services University of the Health Sciences, Bethesda, Maryland 20814, United States*

**Manoj Maniar** – *Onconova Therapeutics, Inc., Newtown, Pennsylvania 18940, United States*

**Amrita K. Cheema** – *Department of Oncology, Lombardi Comprehensive Cancer Center, Georgetown University Medical Center, Washington, District of Columbia 20057, United States; Department of Biochemistry, Molecular and Cellular Biology, Georgetown University Medical Center, Washington, District of Columbia 20057, United States*

Complete contact information is available at:

<https://pubs.acs.org/10.1021/acs.jproteome.2c00458>

### Author Contributions

\*A.D.C. and Y.L. equally contributed to this work.

### Author Contributions

Conceptualization: V.K.S., M.M., A.K.C. Investigation: A.K.C., S.Y.W., O.O.F., A.D.C., Y.L., V.K.S.. Writing—original draft: V.K.S., A.K.C., B.L.J., A.D.C., Y.L., M.M. Revision of the manuscript: V.K.S., A.K.C., A.D.C., Y.L. Funding acquisition: V.K.S. All authors have read and approved the final submitted manuscript. All authors have read and approved the final submitted manuscript.

### Funding

The authors gratefully acknowledge the research support from the Uniformed Services University of the Health Sciences/Armed Forces Radiobiology Research Institute (grant # AFR-B4-10978 AFR-12080) to V.K.S.

### Notes

The opinions or assertions contained herein are the private views of the authors and are not necessarily those of the Uniformed Services University of the Health Sciences or the Department of Defense, USA.

The authors declare no competing financial interest.

The authors report no conflicts of interest. The authors alone are responsible for the content and writing of this paper.

## ACKNOWLEDGMENTS

The authors thank staff of radiation source department for irradiating animals and Dr. Michael Girgis for technical help with LC-MS data acquisition. The Table of Contents graphic is an original graphic that was created by the authors of this manuscript with BioRender.com, and has not been published elsewhere.

## REFERENCES

- (1) Koenig, K. L.; Goans, R. E.; Hatchett, R. J.; Mettler, F. A., Jr; Schumacher, T. A.; Noji, E. K.; Jarrett, D. G. Medical treatment of radiological casualties: current concepts. *Ann. Emerg. Med.* **2005**, *45*, 643–652.
- (2) Ohnishi, T. The disaster at Japan's Fukushima-Daiichi nuclear power plant after the March 11, 2011 earthquake and tsunami, and the resulting spread of radioisotope contamination. *Radiat. Res.* **2012**, *177*, 1–14.
- (3) Williams, J. P.; McBride, W. H. After the bomb drops: a new look at radiation-induced multiple organ dysfunction syndrome (MODS). *Int. J. Radiat. Biol.* **2011**, *87*, 851–868.

- (4) Fushiki, S. Radiation hazards in children - lessons from Chernobyl, Three Mile Island and Fukushima. *Brain Dev.* **2013**, *35*, 220–227.
- (5) Gale, R. P. Medical and policy considerations for nuclear and radiation accidents, incidents and terrorism. *Curr. Opin. Hematol.* **2017**, *24*, 496–501.
- (6) Gale, R. P.; Armitage, J. O. Are we prepared for nuclear terrorism? *N. Engl. J. Med.* **2018**, *378*, 1246–1254.
- (7) Singh, V. K.; Seed, T. M. A review of radiation countermeasures focusing on injury-specific medicinals and regulatory approval status: part I. Radiation sub-syndromes, animal models and FDA-approved countermeasures. *Int. J. Radiat. Biol.* **2017**, *93*, 851–869.
- (8) Singh, V. K.; Seed, T. M. Radiation countermeasures for hematopoietic acute radiation syndrome: growth factors, cytokines and beyond. *Int. J. Radiat. Biol.* **2021**, *97*, 1526–1547.
- (9) Farese, A. M.; MacVittie, T. J. Filgrastim for the treatment of hematopoietic acute radiation syndrome. *Drugs Today* **2015**, *51*, 537–548.
- (10) Hankey, K. G.; Farese, A. M.; Blaauw, E. C.; Gibbs, A. M.; Smith, C. P.; Katz, B. P.; Tong, Y.; Prado, K. L.; MacVittie, T. J. Pegfilgrastim improves survival of lethally irradiated nonhuman primates. *Radiat. Res.* **2015**, *183*, 643–655.
- (11) Singh, V. K.; Seed, T. M. An update on sargramostim for treatment of acute radiation syndrome. *Drugs Today* **2018**, *54*, 679–693.
- (12) Zhong, Y.; Pouliot, M.; Downey, A. M.; Mockbee, C.; Roychowdhury, D.; Wierzbicki, W.; Authier, S. Efficacy of delayed administration of sargramostim up to 120 hours post exposure in a nonhuman primate total body radiation model. *Int. J. Radiat. Biol.* **2021**, *97*, S100–S116.
- (13) Clayton, N. P.; Khan-Malek, R. C.; Dangler, C. A.; Zhang, D.; Asch, A.; Gains, M.; Gardner, B.; Mockbee, C.; Keutzer, J. M.; McManus, J.; et al. Sargramostim (rhu GM-CSF) improves survival of non-human primates with severe bone marrow suppression after acute, high-dose, whole-body irradiation. *Radiat. Res.* **2021**, *195*, 191–199.
- (14) U.S. Food and Drug Administration. *Animal Rule Approvals*; U.S. Food and Drug Administration, 2022. <https://www.fda.gov/drugs/nda-and-bla-approvals/animal-rule-approvals> (accessed July 23, 2022).
- (15) Wong, K.; Chang, P. Y.; Fielden, M.; Downey, A. M.; Bunin, D.; Bakke, J.; Gahagen, J.; Iyer, L.; Doshi, S.; Wierzbicki, W.; Authier, S. Pharmacodynamics of romiplostim alone and in combination with pegfilgrastim on acute radiation-induced thrombocytopenia and neutropenia in non-human primates. *Int. J. Radiat. Biol.* **2020**, *96*, 155–166.
- (16) Wong, K.; Bunin, D. I.; Bujold, K.; Javitz, H. S.; Bakke, J.; Gahagen, J.; Wierzbicki, W.; Andreassen, D. A.; Authier, S.; Chang, P. Y. In *Romiplostim (Nplate) Alone and in Combination with Pegfilgrastim (Neulasta) Increased Survival and Reduces Incidence, Duration, and Severity of Thrombocytopenia Post-Irradiation in Non-Human Primates*, 66th Annual Conference of Radiation Research Society, Virtual, 2020. <https://www.radres.org/events/EventDetails.aspx?id=1336280>.
- (17) Farese, A. M.; Cohen, M. V.; Katz, B. P.; Smith, C. P.; Gibbs, A.; Cohen, D. M.; MacVittie, T. J. Filgrastim improves survival in lethally irradiated nonhuman primates. *Radiat. Res.* **2013**, *179*, 89–100.
- (18) Singh, V. K.; Seed, T. M. An update on romiplostim for treatment of acute radiation syndrome. *Drugs Today* **2022**, *58*, 133–145.
- (19) Gale, R. P.; Armitage, J. O.; Hashmi, S. K. Emergency response to radiological and nuclear accidents and incidents. *Br. J. Haematol.* **2021**, *192*, 968–972.
- (20) Singh, V. K.; Garcia, M.; Seed, T. M. A review of radiation countermeasures focusing on injury-specific medicinals and regulatory approval status: part II. Countermeasures for limited indications, internalized radionuclides, emesis, late effects, and agents demonstrating efficacy in large animals with or without FDA IND status. *Int. J. Radiat. Biol.* **2017**, *93*, 870–884.
- (21) Singh, V. K.; Hanlon, B. K.; Santiago, P. T.; Seed, T. M. A review of radiation countermeasures focusing on injury-specific medicinals and regulatory approval status: part III. Countermeasures under early stages of development along with 'standard of care' medicinal and procedures not requiring regulatory approval for use. *Int. J. Radiat. Biol.* **2017**, *93*, 885–906.
- (22) Ghosh, S. P.; Perkins, M. W.; Hieber, K.; Kulkarni, S.; Kao, T. C.; Reddy, E. P.; Reddy, M. V.; Maniar, M.; Seed, T.; Kumar, K. S. Radiation protection by a new chemical entity, Ex-Rad: efficacy and mechanisms. *Radiat. Res.* **2009**, *171*, 173–179.
- (23) Suman, S.; Datta, K.; Doiron, K.; Ren, C.; Kumar, R.; Taft, D. R.; Fornace, A. J., Jr; Maniar, M. Radioprotective effects of ON 01210.Na upon oral administration. *J. Radiat. Res.* **2012**, *53*, 368–376.
- (24) Ghosh, S. P.; Kulkarni, S.; Perkins, M. W.; Hieber, K.; Pessu, R. L.; Gambles, K.; Maniar, M.; Kao, T. C.; Seed, T. M.; Kumar, K. S. Amelioration of radiation-induced hematopoietic and gastrointestinal damage by Ex-RAD(R) in mice. *J. Radiat. Res.* **2012**, *53*, 526–536.
- (25) Kang, A. D.; Cosenza, S. C.; Bonagura, M.; Manair, M.; Reddy, M. V.; Reddy, E. P. ON01210.Na (Ex-RAD(R)) mitigates radiation damage through activation of the AKT pathway. *PLoS One* **2013**, *8*, No. e58355.
- (26) Suman, S.; Maniar, M.; Fornace, A. J., Jr; Datta, K. Administration of ON 01210.Na after exposure to ionizing radiation protects bone marrow cells by attenuating DNA damage response. *Radiat. Oncol.* **2012**, *7*, No. 6.
- (27) Juntilla, M. M.; Patil, V. D.; Calamito, M.; Joshi, R. P.; Birnbaum, M. J.; Koretzky, G. A. AKT1 and AKT2 maintain hematopoietic stem cell function by regulating reactive oxygen species. *Blood* **2010**, *115*, 4030–4038.
- (28) Li, Y.; Girgis, M.; Wise, S. Y.; Fatanmi, O. O.; Seed, T. M.; Maniar, M.; Cheema, A. K.; Singh, V. K. Analysis of the metabolomic profile in serum of irradiated nonhuman primates treated with Ex-Rad, a radiation countermeasure. *Sci. Rep.* **2021**, *11*, No. 11449.
- (29) Singh, V. K.; Olabisi, A. O. Nonhuman primates as models for the discovery and development of radiation countermeasures. *Expert Opin. Drug Discovery* **2017**, *12*, 695–709.
- (30) Phipps, A. J.; Bergmann, J. N.; Albrecht, M. T.; Singh, V. K.; Homer, M. J. Model for evaluating antimicrobial therapy to prevent life-threatening bacterial infections following exposure to a medically significant radiation dose. *Antimicrob. Agents Chemother.* **2022**, *66*, No. e00546-22.
- (31) National Research Council of the National Academy of Sciences. *Guide for the Care and Use of Laboratory Animals*; National Academies Press, 2011.
- (32) Pannkuk, E. L.; Laiakis, E. C.; Fornace, A. J., Jr; Fatanmi, O. O.; Singh, V. K. A metabolomic serum signature from nonhuman primates treated with a radiation countermeasure, gamma-tocotrienol, and exposed to ionizing radiation. *Health Phys.* **2018**, *115*, 3–11.
- (33) Nagy, V. Accuracy considerations in EPR dosimetry. *Appl. Radiat. Isot.* **2000**, *52*, 1039–1050.
- (34) Singh, V. K.; Kulkarni, S.; Fatanmi, O. O.; Wise, S. Y.; Newman, V. L.; Romaine, P. L.; Hendrickson, H.; Gulani, J.; Ghosh, S. P.; Kumar, K. S.; Hauer-Jensen, M. Radioprotective efficacy of gamma-tocotrienol in nonhuman primates. *Radiat. Res.* **2016**, *185*, 285–298.
- (35) International Standardization Organization and ASTM International. *Standard Practice for Use of an Alanine-EPR Dosimetry System*; ASTM International, ISO and West Conshohocken (US:PA): Geneva, Switzerland, 2013; p 7.
- (36) Girgis, M.; Li, Y.; Ma, J.; Sanda, M.; Wise, S. Y.; Fatanmi, O. O.; Kaytor, M. D.; Cheema, A. K.; Singh, V. K. Comparative proteomic analysis of serum from nonhuman primates administered BIO 300: a promising radiation countermeasure. *Sci. Rep.* **2020**, *10*, No. 19343.
- (37) Musa, A. E.; Shabeeb, D.; Okoro, N. O. E.; Agbele, A. T. Radiation protection by Ex-RAD: a systematic review. *Environ. Sci. Pollut. Res. Int.* **2020**, *27*, No. 33592.

(38) Singh, V. K.; Hauer-Jensen, M. Gamma-tocotrienol as a promising countermeasure for acute radiation syndrome: Current status. *Int. J. Mol. Sci.* **2016**, *17*, No. e663.

(39) Singh, V. K.; Beattie, L. A.; Seed, T. M. Vitamin E: Tocopherols and tocotrienols as potential radiation countermeasures. *J. Radiat. Res.* **2013**, *54*, 973–988.

(40) Singh, V. K.; Seed, T. M. BIO 300: a promising radiation countermeasure under advanced development for acute radiation syndrome and the delayed effects of acute radiation exposure. *Expert Opin. Invest. Drugs* **2020**, *29*, 429–441.

(41) Rosen, E.; Fatanmi, O. O.; Wise, S. Y.; Rao, V. A.; Singh, V. K. Gamma-tocotrienol, a radiation countermeasure, reverses proteomic changes in serum following total-body gamma irradiation in mice. *Sci. Rep.* **2022**, *12*, No. 3387.

(42) Rosen, E.; Fatanmi, O. O.; Wise, S. Y.; Rao, V. A.; Singh, V. K. Tocol prophylaxis for total-body irradiation: A proteomic analysis in murine model. *Health Phys.* **2020**, *119*, 12–20.

(43) Cheema, A. K.; Byrum, S. D.; Sharma, N. K.; Altadill, T.; Kumar, V. P.; Biswas, S.; Balgley, B. M.; Hauer-Jensen, M.; Tackett, A. J.; Ghosh, S. P. Proteomic changes in mouse spleen after radiation-induced injury and its modulation by gamma-tocotrienol. *Radiat. Res.* **2018**, *190*, 449–463.

(44) Kusunoki, Y.; Hayashi, T. Long-lasting alterations of the immune system by ionizing radiation exposure: Implications for disease development among atomic bomb survivors. *Int. J. Radiat. Biol.* **2008**, *84*, 1–14.

(45) Reisz, J. A.; Bansal, N.; Qian, J.; Zhao, W.; Furdai, C. M. Effects of ionizing radiation on biological molecules—mechanisms of damage and emerging methods of detection. *Antioxid. Redox Signaling* **2014**, *21*, 260–292.

(46) Singh, V. K.; Seed, T. M.; Cheema, A. K. Metabolomics-based predictive biomarkers of radiation injury and countermeasure efficacy: Current status and future perspectives. *Expert Rev. Mol. Diagn.* **2021**, *21*, 641–654.

(47) Li, Y.; Girgis, M.; Jayatilake, M.; Serebrenik, A. A.; Cheema, A. K.; Kaytor, M. D.; Singh, V. K. Pharmacokinetic and metabolomic studies with a BIO 300 oral powder formulation in nonhuman primates. *Sci. Rep.* **2022**, *12*, No. 13475.

(48) U.S. Food and Drug Administration. Guidance Document: Product Development under the Animal Rule, 2015. <http://www.fda.gov/downloads/drugs/guidancecomplianceregulatoryinformation/guidances/ucm399217.pdf> (accessed Oct 20, 2022).

(49) U.S. Food and Drug Administration. Animal Rule Information, 2022. <http://www.fda.gov/EmergencyPreparedness/Counterterrorism/MedicalCountermeasures/MCMRegulatoryScience/ucm391604.htm> (accessed Oct 20, 2022).